University of Minho
School of Engineering

Quantum Simulation of spin systems on quantum computers

Irving Leander Reascos Valencia

Project supervised by:

Ph.D. Nuno Miguel Machado Reis Peres

Ph.D. Joaquín Fernández Rossier

March 31, 2023

Contents

Introduction

Motivation

Figure 1: Richard Phillips Feynman (1965). *Source: The Nobel Prize*

$$N = 2^n \text{ (Complex Numbers)}$$

Beyond Classical Capacities [1], [2]

$$n = 50 \to N \approx 10^{15}$$

$$n = 300 \to N \approx 10^{90} > N_{\text{Universe}}$$

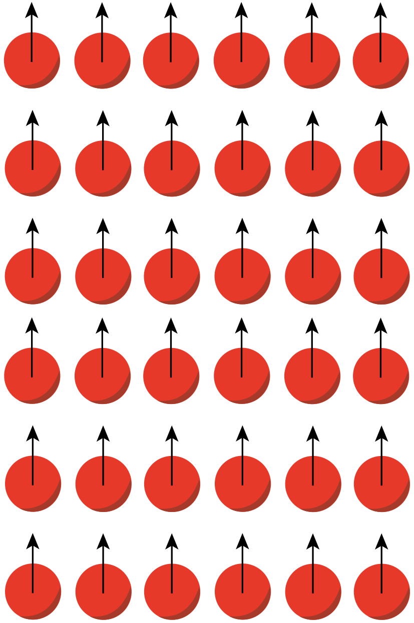

Figure 2: System of n electrons.

Quantum Simulators

Analog Quantum Simulator

$$\hat{\mathrm{H}} \approx \hat{\mathcal{H}}$$

Digital Quantum Simulator

$$\hat{\mathrm{U}}_{\hat{\mathrm{H}}}(t) \approx \hat{\mathrm{U}}_{\hat{\mathcal{H}}}(t)$$

$\hat{\mathcal{H}}$: Target Hamiltonian
$\hat{\mathrm{H}}$: Simulator Hamiltonian

Designing a Quantum Simulation

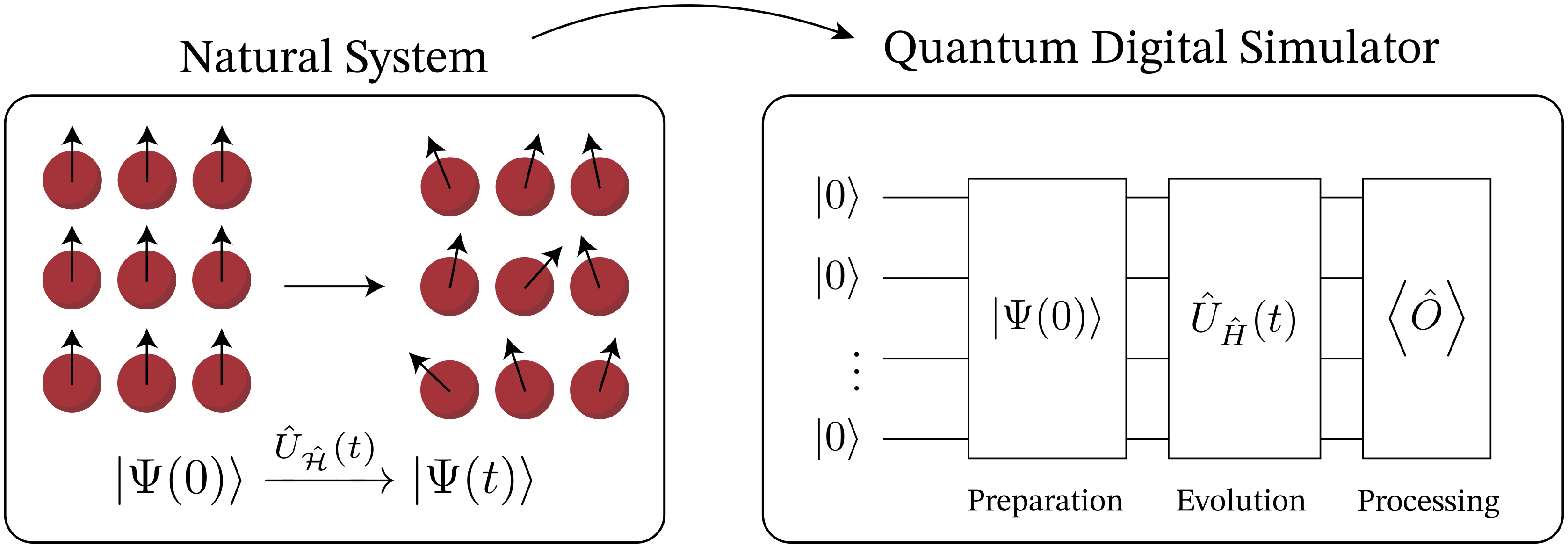

Figure 3: Scheme of digital quantum simulation using a quantum computer.

Spin Systems

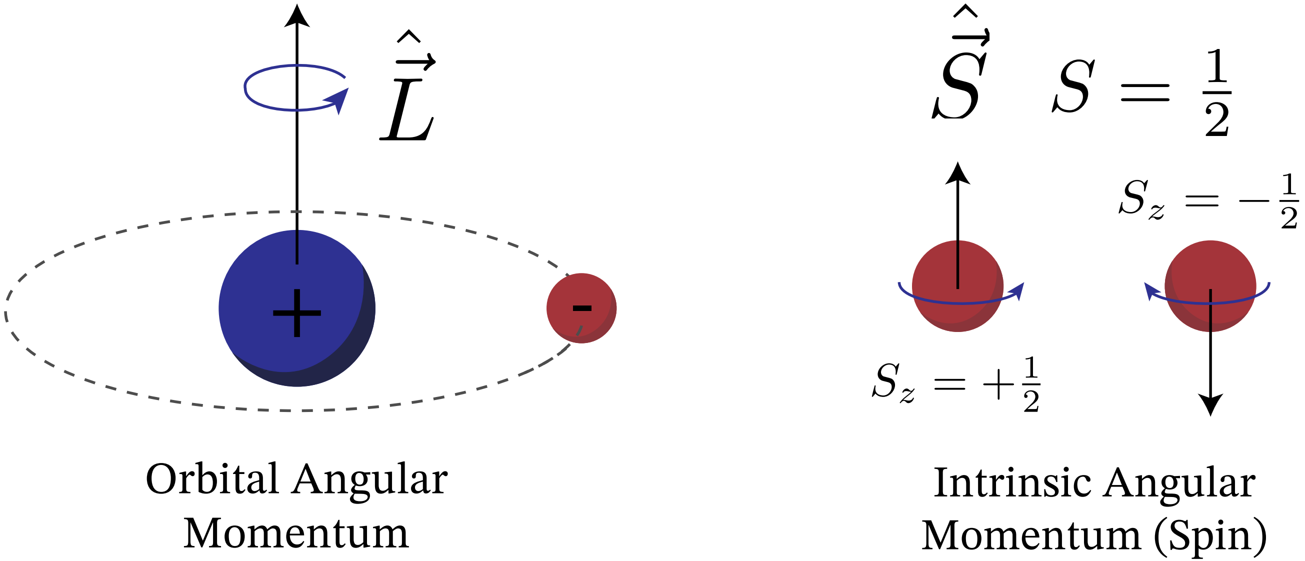

Figure 4: Diagram showing the electron's orbital angular momentum in the hydrogen atom (Left). Diagram illustrating the intrinsic angular momentum (spin) of a particle (Right) [3], [4].

Spin Chirality

Spin Chirality

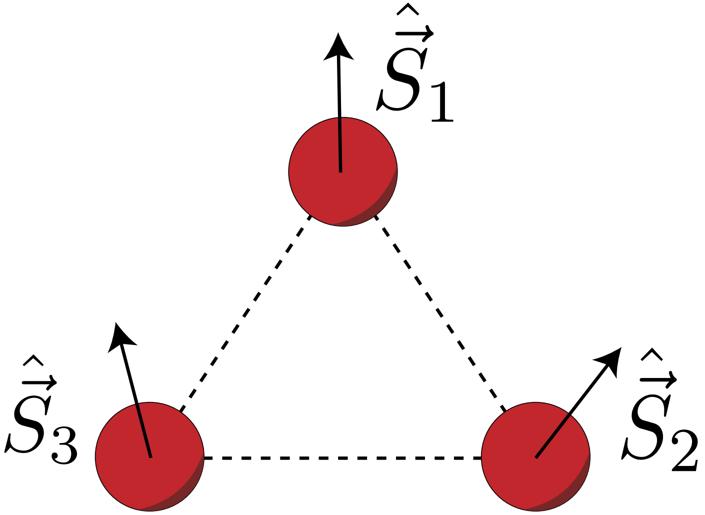

Figure 5: This figure illustrates a spin trimer and its associated spin vector operators.

Chirality Operator [5]

$$\boxed{\hat{\chi} = \vec{\sigma}_1 \cdot \vec{\sigma}_2 \times \vec{\sigma}_3} \tag{1}$$

$$\vec{\sigma}_i = \left(\sigma_x^{(i)}, \sigma_y^{(i)}, \sigma_z^{(i)}\right)^T$$

Chirality eigenstates

$$
\begin{aligned}
\left|\chi = 0, S_z = \tfrac{3}{2}\right\rangle &= \left|\uparrow\uparrow\uparrow\right\rangle \\
\left|\chi = 0, S_z = \tfrac{1}{2}\right\rangle &= \frac{1}{\sqrt{3}}\left(\left|\uparrow\uparrow\downarrow\right\rangle + \left|\uparrow\downarrow\uparrow\right\rangle + \left|\downarrow\uparrow\uparrow\right\rangle \right) \\
\left|\chi = 0, S_z = -\tfrac{1}{2}\right\rangle &= \frac{1}{\sqrt{3}}\left(\left|\downarrow\downarrow\uparrow\right\rangle + \left|\downarrow\uparrow\downarrow\right\rangle + \left|\uparrow\downarrow\downarrow\right\rangle \right) \\
\left|\chi = 0, S_z = -\tfrac{3}{2}\right\rangle &= \left|\downarrow\downarrow\downarrow\right\rangle \\
\left|\chi = -2\sqrt{3}, S_z = \tfrac{1}{2}\right\rangle &= \frac{1}{\sqrt{3}}\left(\left|\uparrow\uparrow\downarrow\right\rangle + \omega\left|\uparrow\downarrow\uparrow\right\rangle + \omega^2\left|\downarrow\uparrow\uparrow\right\rangle \right) \\
\left|\chi = -2\sqrt{3}, S_z = -\tfrac{1}{2}\right\rangle &= \frac{1}{\sqrt{3}}\left(\left|\downarrow\downarrow\uparrow\right\rangle + \omega\left|\downarrow\uparrow\downarrow\right\rangle + \omega^2\left|\uparrow\downarrow\downarrow\right\rangle \right) \\
\left|\chi = 2\sqrt{3}, S_z = \tfrac{1}{2}\right\rangle &= \frac{1}{\sqrt{3}}\left(\left|\uparrow\uparrow\downarrow\right\rangle + \omega^2\left|\uparrow\downarrow\uparrow\right\rangle + \omega\left|\downarrow\uparrow\uparrow\right\rangle \right) \\
\left|\chi = 2\sqrt{3}, S_z = -\tfrac{1}{2}\right\rangle &= \frac{1}{\sqrt{3}}\left(\left|\downarrow\downarrow\uparrow\right\rangle + \omega^2\left|\downarrow\uparrow\downarrow\right\rangle + \omega\left|\uparrow\downarrow\downarrow\right\rangle \right)
\end{aligned}
\tag{2}
$$

$$\omega = e^{i\frac{2\pi}{3}}$$

Computational Basis

$$\boxed{\left|s_1\,s_2\,s_3\right\rangle \rightarrow \left|q_2\,q_1\,q_0\right\rangle}$$

$$\begin{aligned}
\left|\chi=-2\sqrt{3},\, S_z=\tfrac{1}{2}\right\rangle &= \tfrac{1}{\sqrt{3}}\big(\left|100\right\rangle+\omega\left|010\right\rangle+\omega^2\left|001\right\rangle\big)\\
\left|\chi=-2\sqrt{3},\, S_z=-\tfrac{1}{2}\right\rangle &= \tfrac{1}{\sqrt{3}}\big(\left|011\right\rangle+\omega\left|101\right\rangle+\omega^2\left|110\right\rangle\big)\\
\left|\chi=2\sqrt{3},\, S_z=\tfrac{1}{2}\right\rangle &= \tfrac{1}{\sqrt{3}}\big(\left|100\right\rangle+\omega^2\left|010\right\rangle+\omega\left|001\right\rangle\big)\\
\left|\chi=2\sqrt{3},\, S_z=-\tfrac{1}{2}\right\rangle &= \tfrac{1}{\sqrt{3}}\big(\left|011\right\rangle+\omega^2\left|101\right\rangle+\omega\left|110\right\rangle\big)
\end{aligned} \tag{3}$$

$$\omega = e^{i\frac{2\pi}{3}}$$

State $|W\rangle_{N=3}$ [6], [7]

$$G(p) = \begin{pmatrix} \sqrt{p} & -\sqrt{1-p} \\ \sqrt{1-p} & \sqrt{p} \end{pmatrix} \qquad (4)$$

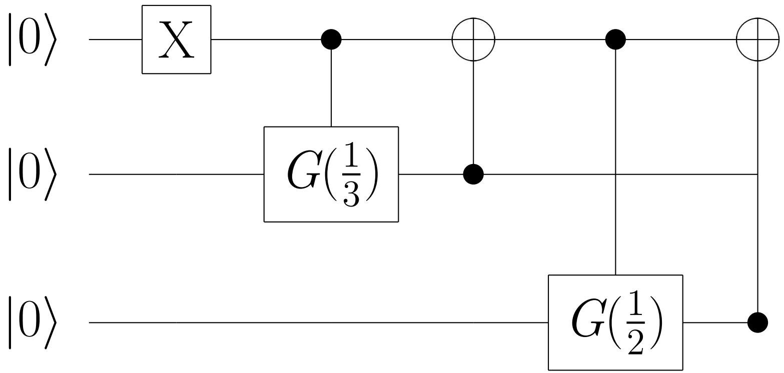

Figure 6: Quantum algorithm to prepare the $|W\rangle_{N=3}$ state.

State Preparation

$$|W\rangle_{N=3} = \frac{1}{\sqrt{N}}\left(|100\rangle + |010\rangle + |001\rangle\right)$$

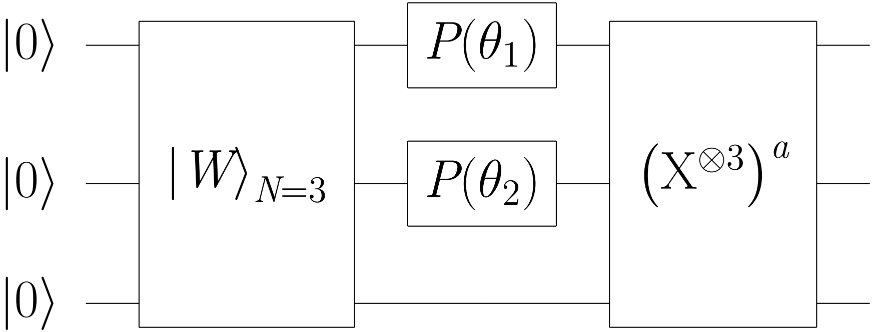

Figure 7: Quantum algorithm to prepare the non-trivial chirality operator eigenstates.

$|\chi, S_z\rangle$ Non-trivial eigenstate

Table 1: Phase gate values for each chirality eigenstate with eigenvalue χ.

χ	$P(\theta_1)$	$P(\theta_2)$
0	0	0
$-2\sqrt{3}$	ω^2	ω
$2\sqrt{3}$	ω	ω^2

$$a = \begin{cases} 1 & \text{if } S_z = -\frac{1}{2} \\ 0 & \text{if } S_z = \frac{1}{2} \end{cases} \tag{5}$$

Chirality Measurement

Chirality Operator $\hat{\chi}$ [8]

$$\begin{aligned}\hat{\chi} &= \vec{\sigma}_1 \cdot \vec{\sigma}_2 \times \vec{\sigma}_3 \\ &= \quad \sigma_x^1 \left(\sigma_y^2 \sigma_z^3 - \sigma_z^2 \sigma_y^3\right) \\ &\quad + \sigma_y^1 \left(-\sigma_x^2 \sigma_z^3 + \sigma_z^2 \sigma_x^3\right) \\ &\quad + \sigma_z^1 \left(\sigma_x^2 \sigma_y^3 - \sigma_y^2 \sigma_x^3\right)\end{aligned}$$

$$\boxed{\begin{aligned}\hat{\chi} &= 2i\left[\hat{P}_i, \hat{P}_{i+1}\right] \\ &= 2i\left(\hat{P}_i \hat{P}_{i+1} - \hat{P}_{i+1} \hat{P}_i\right)\end{aligned}}$$

$$\hat{P}_i = 2^{\left\lfloor \frac{N-1}{2} \right\rfloor} \prod_{j=1}^{\left\lfloor \frac{N-1}{2} \right\rfloor} \left(\vec{S}_{i+j} \cdot \vec{S}_{N+i-j} + \frac{1}{4}\right) \tag{6}$$

$$\hat{P}_i = \prod_{k=0}^{\left\lfloor \frac{N-1}{2} \right\rfloor - 1} SWAP(i+k, i+N-k-2) \tag{7}$$

Operator $\hat{P}_i \hat{P}_{i+1}$

Let's calculate the operators for $i = 1$ and $N = 3$.

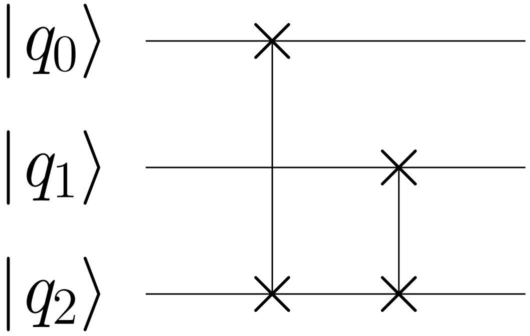

Figure 8: Operator $\hat{P}_1 \hat{P}_2$

$$\hat{P}_1 = SWAP(1,2) \tag{8}$$

$$\hat{P}_2 = SWAP(2,0) \tag{9}$$

$$\boxed{\hat{P}_1 \hat{P}_2 \, |q_2 \;\, q_1 \;\, q_0\rangle = |q_1 \;\, q_0 \;\, q_2\rangle} \tag{10}$$

Linear Combination of Unitaries [9]

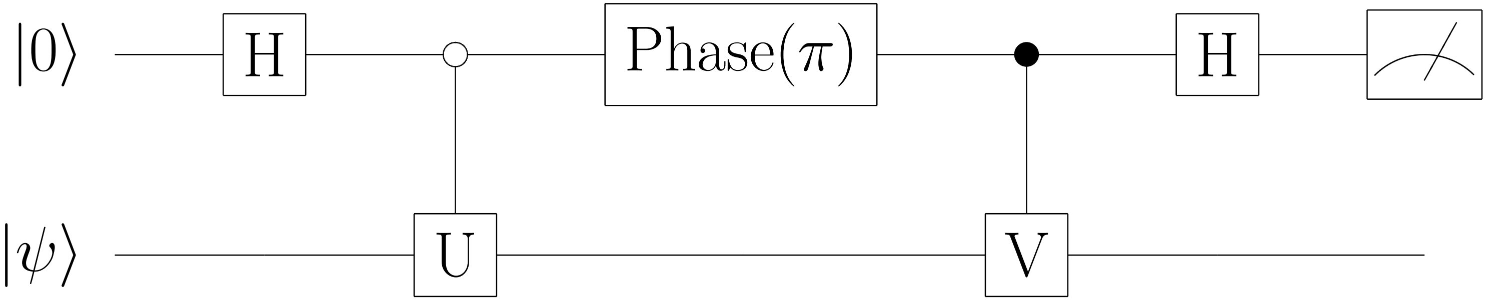

Figure 9: Linear Combination of Unitaries (LCU).

$$\mathrm{LCU}(U, V, \pi)\,|0\psi\rangle = \frac{1}{2}\Big[\,|0\rangle \otimes (U - V)\,|\psi\rangle + |1\rangle \otimes (U + V)\,|\psi\rangle\Big] \tag{11}$$

$\hat{\chi}$ using LCU

$$
\begin{aligned}
\mathrm{LCU}(R, R^\dagger, \pi)\,|0\psi\rangle &= \frac{1}{2}\Big[|0\rangle \otimes \left(R - R^\dagger\right)|\psi\rangle + |1\rangle \otimes \left(R + R^\dagger\right)|\psi\rangle\Big] \\
&= \frac{1}{2}\Big[|0\rangle \otimes \frac{\hat{\chi}}{2i}|\psi\rangle + |1\rangle \otimes \left(R + R^\dagger\right)|\psi\rangle\Big]
\end{aligned} \tag{12}
$$

$$
\begin{aligned}
U &= R = P_1 P_2 \\
V &= R^\dagger = P_2 P_1
\end{aligned} \tag{13}
$$

$$
\hat{\chi} = 2i\left(R - R^\dagger\right) \tag{14}
$$

$$
\mathrm{Probability}(|0\rangle) = \frac{1}{16}\langle\psi|\hat{\chi}^2|\psi\rangle \tag{15}
$$

Results: χ^2

Table 2: The table summarizes the outcomes of 1000 simulations of the LCU method used to measure the value of χ^2. Each simulation is performed with 2^{13} shots.

State	Theoretical χ^2	Simulated
$\lvert\chi = -2\sqrt{3}\rangle$	12	12.00 ± 0.08
$\lvert\chi = 0\rangle$	0	0.0 ± 0.0
$\lvert\chi = 2\sqrt{3}\rangle$	12	12.00 ± 0.08

Indirect Measurement [10]

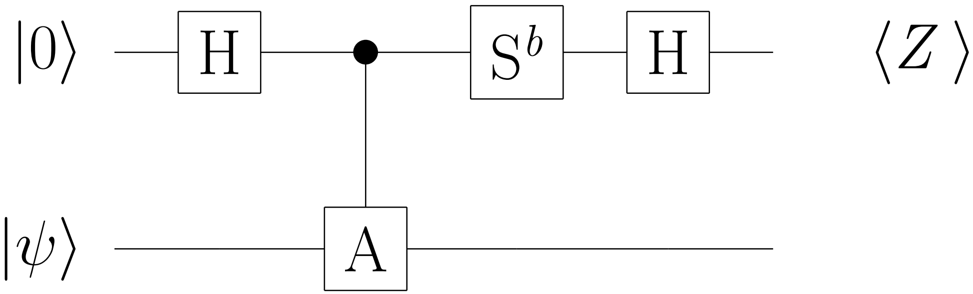

Figure 10: Simplest Hadamard test.

$$\langle Z \rangle = \begin{cases} \mathrm{Re}(\langle\psi|A|\psi\rangle) \ , & b = 0 \\ \mathrm{Im}(\langle\psi|A|\psi\rangle) \ , & b = 1 \end{cases} \tag{16}$$

Hadamard Test and LCU method

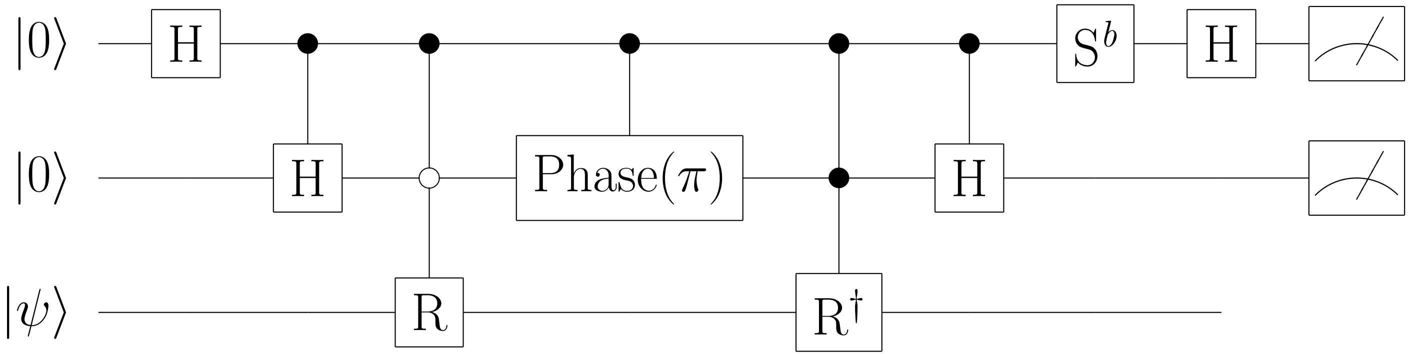

Figure 11: Hadamard test and Linear Combination of Unitaries (LCU) method to measure $\langle \hat{\chi} \rangle$.

$$p_{00} - p_{10} = \begin{cases} \frac{1}{4} \langle \psi | \mathrm{Im}\{\hat{\chi}\} | \psi \rangle \,, & b = 0 \\ \frac{1}{4} \langle \psi | \mathrm{Re}\{\hat{\chi}\} | \psi \rangle \,, & b = 1 \end{cases} \tag{17}$$

Results: $\mathrm{Re}\left\{\hat{\chi}\right\}$

Table 3: The table summarizes the outcomes of 1000 simulations to measure the value of χ. Each simulation is performed with 2^{13} shots.

State	Theoretical χ	Simulated
$\lvert\chi = -2\sqrt{3}\rangle$	$-2\sqrt{3} \approx -3.46$	-3.46 ± 0.02
$\lvert\chi = 0\rangle$	0	0.00 ± 0.03
$\lvert\chi = 2\sqrt{3}\rangle$	$2\sqrt{3} \approx 3.46$	3.46 ± 0.02

Quantum Phase Estimation (QPE)

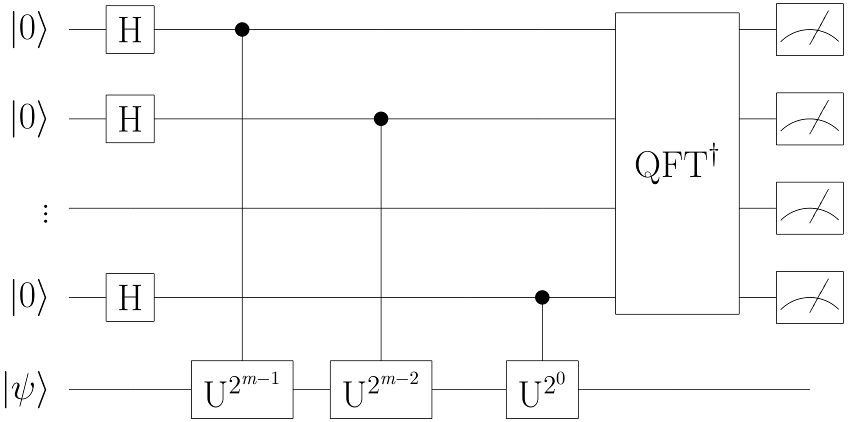

Figure 12: Quantum Phase Estimation.

$$U|\psi\rangle = e^{2\pi i\theta}|\psi\rangle \tag{18}$$

$$QPE(U)|\psi\rangle \rightarrow |2^m\theta\rangle \tag{19}$$

Chirality Time Evolution Operator

$$\begin{aligned}\hat{\chi} &= \vec{\sigma}_1 \cdot \vec{\sigma}_2 \times \vec{\sigma}_3 \\ &= \sigma_x^1 \left(\sigma_y^2\sigma_z^3 - \sigma_z^2\sigma_y^3\right) + \sigma_y^1 \left(-\sigma_x^2\sigma_z^3 + \sigma_z^2\sigma_x^3\right) + \sigma_z^1 \left(\sigma_x^2\sigma_y^3 - \sigma_y^2\sigma_x^3\right)\end{aligned} \tag{20}$$

$$\hat{U}_\chi(t) = e^{-it\hat{\chi}} = \lim_{n\to\infty} \left(\prod_{j,k,l} \exp\left\{ -i\,\frac{t}{n}\,\epsilon_{jkl}\,\sigma_j^1\sigma_k^2\sigma_l^3 \right\} \right)^n \tag{21}$$

$QPE(\hat{U}_\chi(t))$

$$e^{2\pi i\theta} = e^{-it\chi}$$

$$2\pi i\theta = 2\pi - t\chi$$

$$\boxed{\theta = \left(1 - \frac{t\chi}{2\pi}\right) \mathrm{mod}(1)} \tag{22}$$

We want to distinguish 3 eigenvalues, positive, negative and zero.

$$m \geq \log_2(3) \approx 1.58$$

$$\boxed{m = 2} \quad \text{Ancillary qubits} \tag{23}$$

Applying $\hat{U}_\chi(t)$ to Basis States

The application of the time evolution operator to the computational basis state yields the following results.

$$\hat{U}_\chi(t)\left|100\right\rangle = c_0(t)\left|100\right\rangle + c_1\left|010\right\rangle + c_{-1}\left|001\right\rangle \tag{24}$$

$$\boxed{c_j(t) = \frac{1}{3} + \frac{2}{3}\cos\left(2\sqrt{3}t + j\frac{2\pi}{3}\right)} \tag{25}$$

Simplifying $\hat{U}_\chi(t)$

$$\hat{U}_\chi(t)\left|100\right\rangle = c_0(t)\left|100\right\rangle + c_1(t)\left|010\right\rangle + c_{-1}(t)\left|001\right\rangle \tag{26}$$

$$\boxed{c_j(t) = \frac{1}{3} + \frac{2}{3}\cos\left(2\sqrt{3}t + j\frac{2\pi}{3}\right)} \tag{27}$$

If $t = T = \frac{2\pi}{3}\frac{1}{2\sqrt{3}}$, then

$$c_{-1}(T) = 1, \quad c_0(T) = 0, \quad c_1(T) = 0 \tag{28}$$

$$\boxed{\hat{U}_\chi(T)\left|q_2\ q_1\ q_0\right\rangle = \left|q_1\ q_0\ q_2\right\rangle} \tag{29}$$

Hadamard Test $\hat{U}_{\chi}(T)$

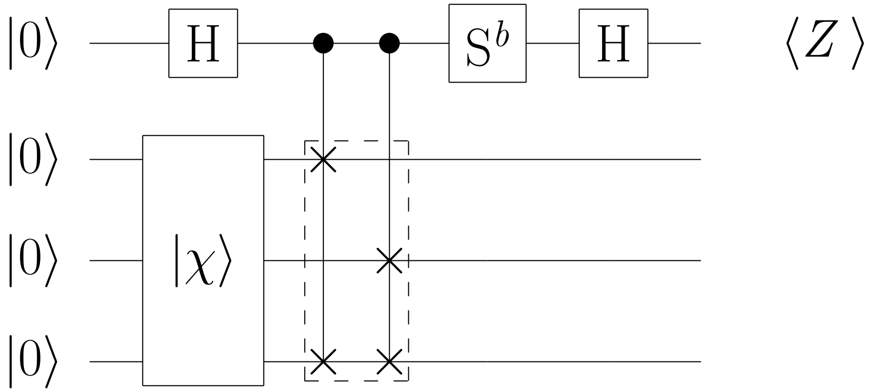

Figure 13: Hadamard test of $\hat{U}_{\chi}(T)$.

$$\langle Z \rangle = \begin{cases} \cos(T\chi), & b = 0 \\ \sin(T\chi), & b = 1 \end{cases} \tag{30}$$

Cycle test to measure Bargmann invariants [11].

Results: Hadamard Test $\hat{U}_\chi(T)$

Table 4: The table summarizes the outcomes of 1000 simulations to measure the value of χ. Each simulation is performed with 2^{13} shots.

State	Theoretical χ	Simulated
$\lvert\chi = -2\sqrt{3}\rangle$	$-2\sqrt{3} \approx -3.46$	-3.46 ± 0.04
$\lvert\chi = 0\rangle$	0	0.00 ± 0.03
$\lvert\chi = 2\sqrt{3}\rangle$	$2\sqrt{3} \approx 3.46$	3.46 ± 0.04

$QPE(\hat{U}_\chi(T))$

$$\theta = \left(1 - \frac{T\chi}{2\pi}\right) \mathrm{mod}(1), \quad T = \frac{2\pi}{3} \frac{1}{2\sqrt{3}} \tag{31}$$

$$\theta = \begin{cases} \frac{1}{3}, & \chi = -2\sqrt{3} \\ 0, & \chi = 0 \\ \frac{2}{3}, & \chi = 2\sqrt{3} \end{cases} \tag{32}$$

Results: $QPE(\hat{U}_\chi(T))$

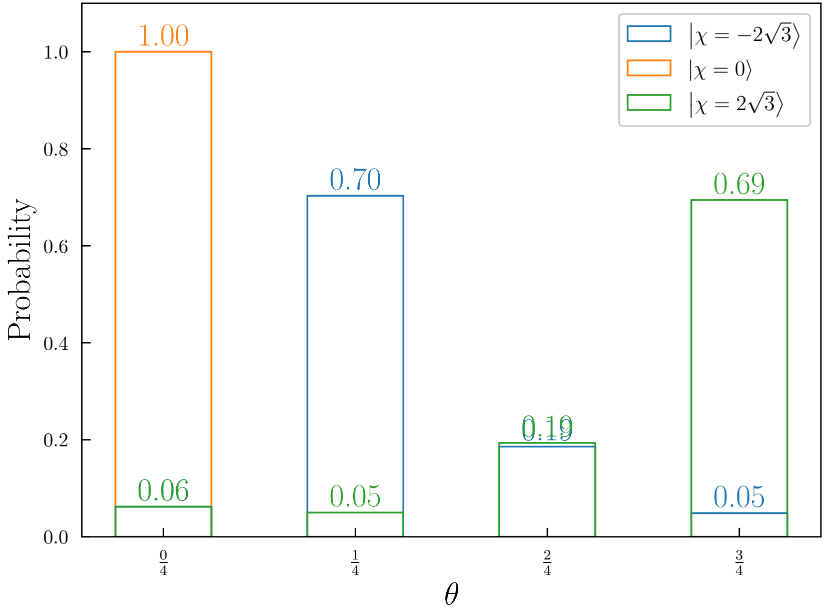

Figure 14: The graphic summarizes the outcomes of the simulation with 2^{13} shots to measure θ.

Table 5: Each state's theoretical result is presented in the table.

State	Theoretical θ	Measured
$\lvert\chi = -2\sqrt{3}\rangle$	$\frac{1}{3} \approx 0.3\overline{3}$	0.25
$\lvert\chi = 0\rangle$	0	0
$\lvert\chi = 2\sqrt{3}\rangle$	$\frac{2}{3} \approx 0.6\overline{6}$	0.75

Results: Trotterized $QPE(\hat{U}_\chi(T))$

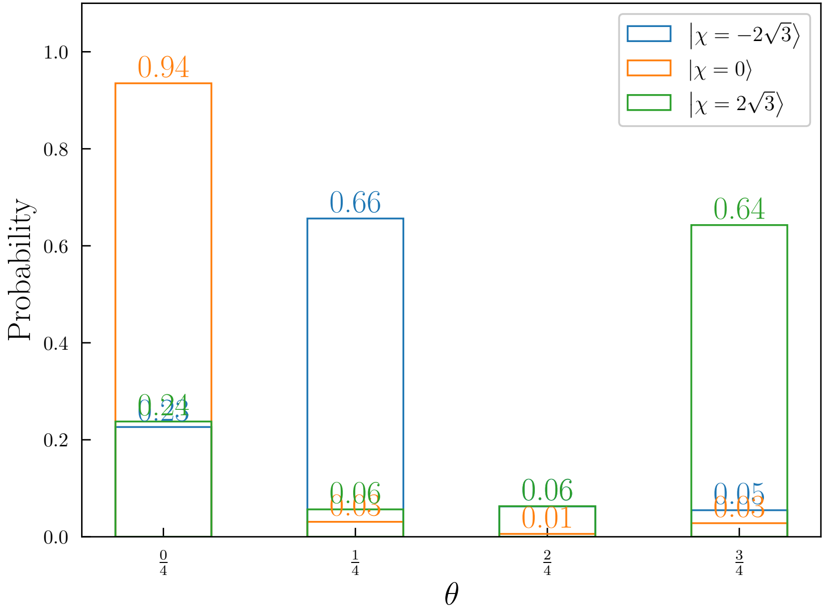

Figure 15: The graphic summarizes the outcomes of the simulation with 2^{13} shots to measure θ. This simulation used 1 trotter layer.

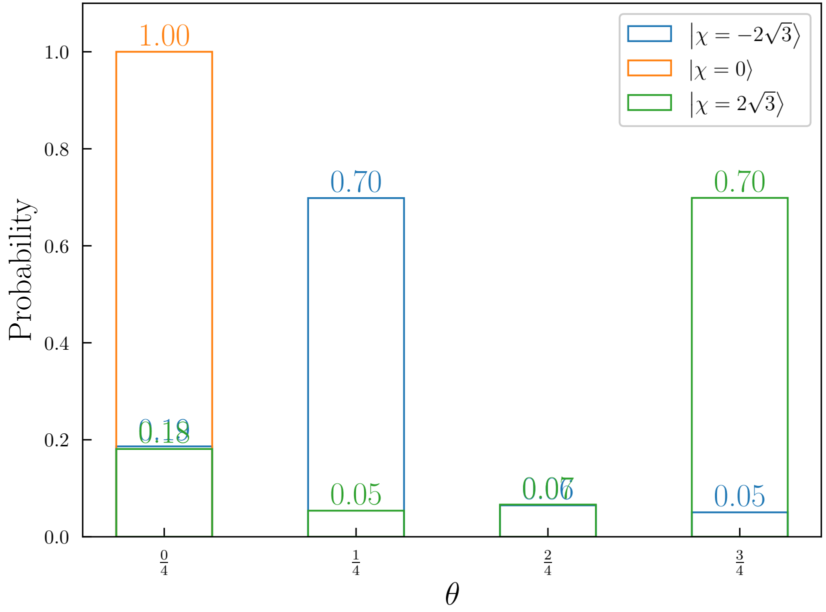

Figure 16: The graphic summarizes the outcomes of the simulation with 2^{13} shots to measure θ. This simulation used 100 trotter layers.

Conclusions

Conclusions

- Successfully implemented the chirality eigenstates.
- Successfully developed quantum algorithms for measuring the chirality property of a given state without destroying it.
- The algorithms utilize different techniques including Hadamard Test, LCU, QPE, and Trotterization.

Future Work

- Analyze and compare the algorithms.
- Implement an alternative spin system.
- Improve the algorithms with respect to gate count.
- Test the algorithms on a physical NISQ device.

Thank you for your attention

University of Minho School of Engineering

INL INTERNATIONAL IBERIAN NANOTECHNOLOGY LABORATORY

FUNDAÇÃO CALOUSTE GULBENKIAN

References I

[1] S. Lloyd, "Universal quantum simulators," *Science*, vol. 273, no. 5278, pp. 1073–1078, Aug. 23, 1996, ISSN: 0036-8075, 1095-9203. DOI: 10.1126/science.273.5278.1073. [Online]. Available: https://www.science.org/doi/10.1126/science.273.5278.1073 (visited on 12/09/2022).

[2] A. J. Daley, I. Bloch, C. Kokail, *et al.*, "Practical quantum advantage in quantum simulation," *Nature*, vol. 607, no. 7920, pp. 667–676, Jul. 2022, Number: 7920 Publisher: Nature Publishing Group, ISSN: 1476-4687. DOI: 10.1038/s41586-022-04940-6. [Online]. Available: https://www.nature.com/articles/s41586-022-04940-6 (visited on 12/14/2022).

References II

[3] J. Parkinson and D. J. J. Farnell, *An Introduction to Quantum Spin Systems* (Lecture Notes in Physics). Berlin, Heidelberg: Springer Berlin Heidelberg, 2010, vol. 816, ISBN: 978-3-642-13289-6 978-3-642-13290-2. DOI: 10.1007/978-3-642-13290-2. [Online]. Available: http://link.springer.com/10.1007/978-3-642-13290-2 (visited on 10/19/2022).

[4] J. J. Sakurai and E. D. Commins, *Modern quantum mechanics, revised edition*, 1995.

References III

[5] X. G. Wen, F. Wilczek, and A. Zee, "Chiral spin states and superconductivity," *Physical Review B*, vol. 39, no. 16, pp. 11 413–11 423, Jun. 1, 1989, ISSN: 0163-1829. DOI: 10.1103/PhysRevB.39.11413. [Online]. Available: https://link.aps.org/doi/10.1103/PhysRevB.39.11413 (visited on 10/17/2022).

References IV

[6] D. Cruz, R. Fournier, F. Gremion, *et al.*, "Efficient quantum algorithms for ghz and w states, and implementation on the ibm quantum computer," *Advanced Quantum Technologies*, vol. 2, no. 5-6, p. 1 900 015, 2019. DOI: https://doi.org/10.1002/qute.201900015. eprint: https://onlinelibrary.wiley.com/doi/pdf/10.1002/qute.201900015. [Online]. Available: https://onlinelibrary.wiley.com/doi/abs/10.1002/qute.201900015.

[7] B. Murta, P. M. Q. Cruz, and J. Fernández-Rossier, *Preparing valence-bond-solid states on noisy intermediate-scale quantum computers*, 2022. arXiv: 2207.07725 [quant-ph].

References V

[8] V. Subrahmanyam, "Chirality operators for heisenberg spin systems," *Physical Review B*, vol. 50, no. 9, pp. 6468–6470, Sep. 1, 1994, ISSN: 0163-1829, 1095-3795. DOI: 10.1103/PhysRevB.50.6468. [Online]. Available: https://link.aps.org/doi/10.1103/PhysRevB.50.6468 (visited on 10/17/2022).

[9] A. M. Childs and N. Wiebe, "Hamiltonian simulation using linear combinations of unitary operations," *arXiv preprint arXiv:1202.5822*, 2012.

[10] K. Mitarai and K. Fujii, "Methodology for replacing indirect measurements with direct measurements," *Physical Review Research*, vol. 1, no. 1, p. 013 006, 2019.

References VI

[11] M. Oszmaniec, D. J. Brod, and E. F. Galvão, *Measuring relational information between quantum states, and applications*, 2021. arXiv: 2109.10006 [quant-ph].

[12] D.-W. Wang, C. Song, W. Feng, *et al.*, "Synthesis of antisymmetric spin exchange interaction and chiral spin clusters in superconducting circuits," *Nature Physics*, vol. 15, no. 4, pp. 382–386, Apr. 2019, ISSN: 1745-2473, 1745-2481. DOI: 10.1038/s41567-018-0400-9. [Online]. Available: http://www.nature.com/articles/s41567-018-0400-9 (visited on 10/17/2022).